Cancer Immunology, Immunotherapy (2022) 71:2433–2448
https://doi.org/10.1007/s00262-022-03172-x

ORIGINAL ARTICLE

Enhancement of CD70-specific CAR T treatment by IFN-γ released from oHSV-1-infected glioblastoma

Guidong Zhu[1,2,3,4] · Junwen Zhang[1,2,3] · Qing Zhang[1,2,3] · Guishan Jin[1,2,3] · Xiaodong Su[1,2,3] · Sisi Liu[5] · Fusheng Liu[1,2,3]

Received: 7 July 2021 / Accepted: 11 February 2022 / Published online: 6 March 2022

Abstract

Even with progressive combination treatments, the prognosis of patients with glioblastoma (GBM) remains extremely poor. OV is one of the new promising therapeutic strategies to treat human GBM. OVs stimulate immune cells to release cytokines such as IFN-γ during oncolysis, further improve tumor microenvironment (TME) and enhance therapeutic efficacy. IFN-γ plays vital role in the apoptosis of tumor cells and recruitment of tumor-infiltrating T cells. We hypothesized that oncolytic herpes simplex virus-1 (oHSV-1) enhanced the antitumor efficacy of novel CD70-specific chimeric antigen receptor (CAR) T cells by T cell infiltration and IFN-γ release. In this study, oHSV-1 has the potential to stimulate IFN-γ secretion of tumor cells rather than T cell secretion and lead to an increase of T cell activity, as well as CD70-specific CAR T cells can specifically recognize and kill tumor cells in vitro. Specifically, combinational therapy with CD70-specific CAR T and oHSV-1 promotes tumor degradation by enhancing pro-inflammatory circumstances and reducing anti-inflammatory factors in vitro. More importantly, combined therapy generated potent antitumor efficacy, increased the proportion of T cells and natural killer cells in TME, and reduced regulatory T cells and transformed growth factor-β1 expression in orthotopic xenotransplanted animal model of GBM. In summary, we reveal that oHSV-1 enhance the therapeutic efficacy of CD70-spefific CAR T cells by intratumoral T cell infiltration and IFN-γ release, supporting the use of CAR T therapy in GBM therapeutic strategies.

Keywords CD70 · Chimeric antigen receptor · Glioblastoma · Oncolytic herpes simplex virus-1 · Immunotherapy · Tumor microenvironment

Abbreviations

CAR	Chimeric antigen receptor
DAPI	2-(4-Amidinophenyl)-6-indolecarbamidine dihydrochloride.
DMEM	Dulbecco's modified eagle medium
EGFP	Enhanced green fluorescent protein
GBM	Glioblastoma
IF	Immunofluorescence
IFN	Interferon
IL	Interleukin
IVIS	In vivo imaging system
NK	Natural killer
PBMCs	Peripheral blood mononuclear cells
PBS	Phosphate buffer saline
oHSV-1	Oncolytic herpes simplex virus-1
OVs	Oncolytic virus
TGF	Transforming growth factor
TME	Tumor microenvironment
TNF	Tumor necrosis factor
trCD27	Truncated CD27
Treg	Regulatory T
SME	Scanning electron microscopy

✉ Fusheng Liu
liufusheng@ccmu.edu.cn; liufushengs@hotmail.com

1 Brain Tumor Research Center, Beijing Neurosurgical Institute, Capital Medical University, Beijing 100070, China

2 Department of Neurosurgery, Beijing Tiantan Hospital Affiliated To Capital Medical University, Beijing 100070, China

3 Beijing Laboratory of Biomedical Materials, Beijing 100070, China

4 Shandong Second Provincial General Hospital, Shandong Provincial ENT Hospital, Jinan 250031, China

5 Beijing Tongren Eye Center, Beijing Ophthalmology & Visual Sciences Key Lab, Beijing Tongren Hospital, Capital Medical University, Beijing, China

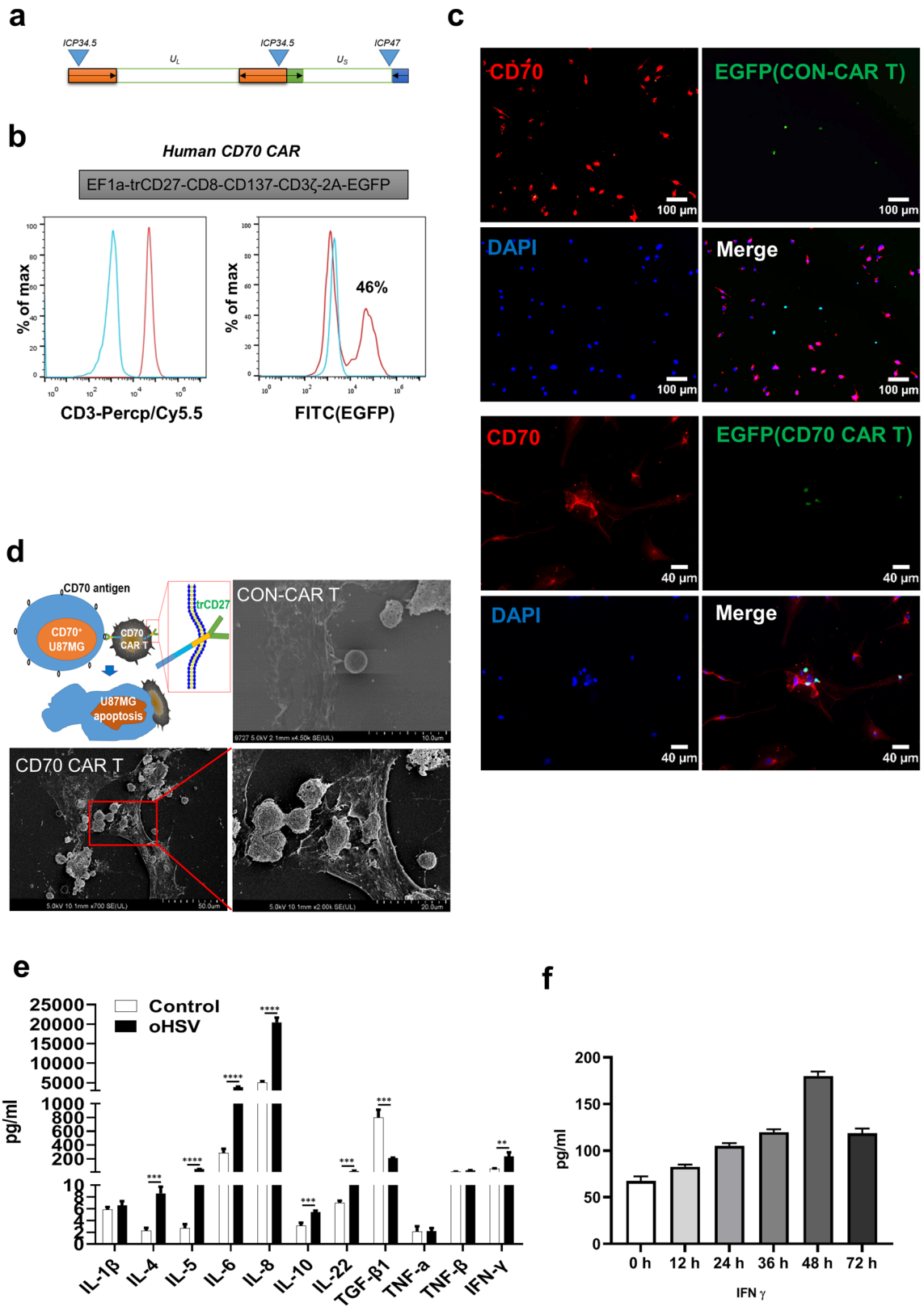
a
ICP34.5
ICP34.5
ICP47
U_L
U_S
b
Human CD70 CAR
EF1a-trCD27-CD8-CD137-CD3ζ-2A-EGFP
% of max
CD3-Percp/Cy5.5
46%
FITC(EGFP)
c
CD70
EGFP(CON-CAR T)
DAPI
Merge
100 μm
CD70
EGFP(CD70 CAR T)
40 μm
d
CD70 antigen
CD70+ U87MG
CD70 CAR T
trCD27
U87MG apoptosis
CON-CAR T
CD70 CAR T
e
Control
oHSV
pg/ml
IL-1β
IL-4
IL-5
IL-6
IL-8
IL-10
IL-22
TGF-β1
TNF-a
TNF-β
IFN-γ
f
pg/ml
0 h
12 h
24 h
36 h
48 h
72 h
IFN γ

◂**Fig. 1** Recognition of GBM by CD70-specific CAR T cells and secretion of factors in supernatants from oHSV-1-infected GBM. **a** Diagram of genetically modified oHSV. **b** Construction and identification of human CD70 CAR T cells. Human-derived EF1a-trCD27-CD8-CD137-CD3ζ-2A-EGFP was a lentivirus-based vector (GV401) encoding truncated CD27 for antigen recognition and transmembrane domains. Flow cytometry detected that the purity of isolated T cells was more than 98% and CD70 CAR T cells with a positive rate of 46%. **c** CD70 CAR T cells specifically recognized GBM expressing CD70 in vitro**.** Human CAR T cells were cocultured with U87 for 12 h, immunofluorescence staining were performed. Fluorescence microscope obtained the images. **d** The pattern and electron microscopy of CAR T cells capture tumor cells and attack them. After the CAR T cells approach and recognize the tumor cells, they gather toward the tumor cells and approach each other, and then stretch out pseudopods to capture the tumor cells. **e** Luminex assay examined secretion of different cytokines in conditioned media from oHSV-1-infected GBM. **F** The levels of IFN-γ at different time point were measured by ELISA. All experiments were performed at least three times. $^{**}P<0.01$, $^{***}P<0.001$, $^{****}P<0.0001$ by 1-way ANOVA with Tukey's post-hoc test

Introduction

Glioma is an aggressive malignant tumor with a poor prognosis. Recent phase III trials of new strategies for glioblastoma (GBM), such as anti-angiogenic drugs, new chemotherapeutic agents, oncolytic virus (OVs) local injections, targeted drugs, checkpoint inhibitors, and immunotherapy regimens have made significant progress. But it is still limited [1–3]. New treatment methods and alternative strategies are urgently needed.

OVs kill tumors while providing the necessary danger signals to activate the immune system [4]. OVs rely on the dual-action mechanism of selectively killing tumor cells and inducing a systemic antitumor immune response to achieve therapeutic purposes [5]. These characteristics make OVs an excellent potential partner for synergy with emerging immunotherapy [6–8].

With the development of immunotherapy in recent years and the success of chimeric antigen receptor (CAR) T-cell immunotherapy in the treatment of $CD19^+$ acute lymphoblastic leukemia [9], immunotherapy using synthetic CAR to redirect T cells to recognize specific antigens expressed on the surface of tumor cells carries the hope of curing tumors. However, in solid tumors, due to the lack of ideal targets like CD19, tumor heterogeneity, escape of tumor antigens [10], and the inhibition of T-cell infiltration and function by an immunosuppressed tumor microenvironment (TME) [11–13], CAR T-cell therapy is challenging [14–20]. To further improve the efficacy, tumor antigens need to be identified and verified in the most challenging malignant tumors, such as gliomas. In particular, the highly immunosuppressed TME of gliomas limits T-cell infiltration and induces T-cell dysfunction. Therefore, finding a suitable target and reversing the immunosuppressive TME provides new ideas for glioma treatment.

CD70 is the only ligand of CD27, a glycosylated transmembrane protein of the tumor necrosis factor (TNF) receptor family [21]. CD70 expression is limited to highly activated T/B lymphocytes and a small percentage of mature dendritic cells, but CD70 expression cannot be detected in 52 normal tissues from different organs [22]. Presently, CD70 overexpression types have been reported in various malignant tumors [23]. Our immunohistochemical analysis of specimens from 63 patients with GBM shows that 20.6% of GBMs expressed high CD70. In particular, the promising results obtained in the experimental mouse model of glioma (showing a robust antitumor effect) have made CD70 an ideal target for CAR T cells in some gliomas, with little extratumor toxicity [22].

Here, we combined engineering oncolytic herpes simplex virus-1 (oHSV-1) with selective replication and CAR T cells targeting CD70. We demonstrate that oHSV-1 can enhance T-cell function and infiltration, further reverse the highly immunosuppressive tumor microenvironment to improve the efficacy of CAR T-cell immunotherapy.

Methods

Construction of engineering oHSV-1

Oncolytic HSV-1 was provided by Dr. Zhang Junwen from the Beijing Neurosurgical Institute. Wild-type HSV-1 (F) was genetically modified by genetic engineering. The neurocytotoxic gene (γ34.5) and ICP47 gene in the virus were deleted by genetic engineering (Fig. 1a). The infectivity of the final experimental-grade virus preparation was determined. After testing to determine that the virus preparations were contamination free, the virus solutions were divided into aliquots and stored at −80 °C to avoid repeated freezing and thawing. The viruses were propagated in 293T cells, and the titer was expressed as pfu/ml, as assessed using the TCID50 method [24, 25].

Construction of human CD70 CAR T cells

As described above [22, 26], a human truncated CD27 (trCD27)-2ndCAR lentiviral vector containing a trCD27 (including extracellular portion of CD27, aa1-191), CD8 transmembrane domain, and a CD137 costimulatory domain and CD3-zeta was generated (Fig. 1b; EF1a-trCD27-CD8-CD137-CD3ζ-2A-EGFP). T cells from healthy donors were transduced with lentivirus overexpressing anti-CD70 CAR. Uninfected T cells activated under the same conditions were used as a control. The short process was performed as follows. First, we subcloned trCD27-2ndCAR into a vector

(Jikai Gene Chemical Technology Co., Ltd., Shanghai, China) and packaged it in 293 T cells using a self-inactivating three-plasmid lentiviral packaging system to obtain trCD27-2ndCAR overexpression lentivirus. For T cell transduction, the peripheral blood of healthy donors was collected (The peripheral blood sample donors had signed the written informed consent), and peripheral blood mononuclear cells (PBMCs) were isolated using Lymphoprep (StemCell Technologies, Vancouver, BC, Canada), the EasySep™ Direct Human T Cell Isolation Kit (StemCell Technologies, Vancouver, BC, Canada), EasySep™ Magnet (StemCell Technologies, Vancouver, BC, Canada), and other purified T cells. Anti-CD3/CD28/CD2 ImmunoCult™ Human T Cell Activator (StemCell Technologies, Vancouver, BC, Canada) was added to the ImmunoCult ™-XF T Cell Expansion Medium (StemCell Technologies, Vancouver, BC, Canada) at a concentration of 25 µl/ml to activate human T cells. The activated T cells were stained with human CD3 Mouse mAb-PerCP/Cy5.5 (StemCell Technologies, Vancouver, BC, Canada), and BD Accuri C6 Plus flow cytometry (BD Biosciences, San Jose, CA, USA) was used to identify the purity of the T cells. The isotype negative control antibody was the human IgG isotype (Abcam, Cambridge, MA, USA). After 48 h, the activated T cells were seeded in a 12-well plate precoated with Retronectin (TAKARA, Tokyo, Japan) and were transduced by the lentiviral vector overexpressing trCD27-2ndCAR (MOI = 10). The above processes were all performed according to the manufacturer's instructions. Five days after transduction, CD70 CAR T cells were harvested for subsequent *in vitro* and *in vivo* experiments. Negative CAR T cells as control (Con-CAR T). Un-transduction T (NT) cells as control.

CD70 GBM cell line

A previous study confirmed that U87MG cells positively express CD70 [22]. To obtain U87MG-Luc cells, the lentiviral vector Lenti-CMV-Puro-Luc used to transduce U87MG was designed and synthesized by Shanghai Jikai Gene Chemical Technology Co., Ltd. U87MG cells were infected with Lenti-CMV-Puro-Luc (MOI = 2) and cultured for 6 h. Three days after infection, 1 µg/ml of puromycin (Sigma-Aldrich, St. Louis, MO, USA) was added to Dulbecco's Modified Eagle Medium (DMEM) (GIBCO BRL, Grand Island, NY, USA) containing 10% fetal bovine serum (GIBCO BRL, Grand Island, NY, USA). U87MG-Luc cells were cultured in DMEM supplemented with 10% fetal bovine serum.

CAR T cell tumor recognition and improve therapeutic efficacy

Human CAR T cells were cocultured with human GBM cell lines. After 12 h, immunofluorescence staining and scanning electron microscopy (SEM) were performed. For immunofluorescence staining, primary antibody mouse anti-human CD70 (Abcam, Cambridge, MA, USA) and secondary antibody goat Anti-Mouse IgG H&L (DyLight® 594) (Abcam, Cambridge, MA, USA) were used. The fluorescence was recorded using an inverted fluorescence microscope (Carl Zeiss, Jena, Germany). The samples were prepared by coating with Pt using sputtering before SEM observation. SEM was performed using SU8000 SEM (Hitachi, Tokyo, Japan) at 5 kV. The samples were analyzed according to the manufacturer's instructions for immunofluorescence and SEM.

To determine the killing capacity of the combination therapy, we inoculated GBM cells (10^4) in 96-well plates and added oHSV-1 with an MOI of 0.2 for infection or control medium. After 24 h, CD70 CAR T cells or control T cells were added at effector/target ratios of 1:1, 1:2, and 1:4. D-luciferase was added at 12 h, 24 h, and 48 h, and in vitro bioluminescence imaging was performed using the in vivo imaging system (IVIS) Spectrum (Perkin-Elmer, Waltham, MA, USA). Data analysis was performed using Spectrum Living Image software (version 4.0).

Magnetic Luminex assays

Magnetic Luminex® Assay was a magnetic bead-based antibody microarray founded upon the sandwich immunoassay principle, which was used to assess the levels of biomarkers in a single sample. In our study, we custom-made a unique blend of magnetic bead cytokines panel including pro-inflammatory and anti-inflammatory factors to screen biomarkers. All procedures were performed as described in the manufacturer's instructions. Each well absorbance was determined at 450 nm. Data were analyzed by 5-parameter curve fitting using Bio-Plex Manager software, version 6.1.1.

ELISA

The levels of interleukin (IL)-6, IL-8, TNF-α, TNF-β1, transforming growth factor (TGF)-β1, IL-4, IL-10, and interferon (IFN)-γ in the different supernatants were measured using Human ELISA kits (Neobioscience, China) according to the manufacturer's instructions.

Animal experiment ethics and welfare

The Experimental Animal Welfare and Ethics Committee of Beijing Tiantan Hospital affiliated to Capital Medical University reviewed and approved all the animal experiments. All the animal procedures were performed in the animal facilities of Beijing Tiantan Hospital affiliated to Capital Medical University and were conducted strictly according to the protocols approved by the Experimental Animal Welfare and Ethics Committee. Animal survival was monitored daily. The animals were humanely killed at a predetermined

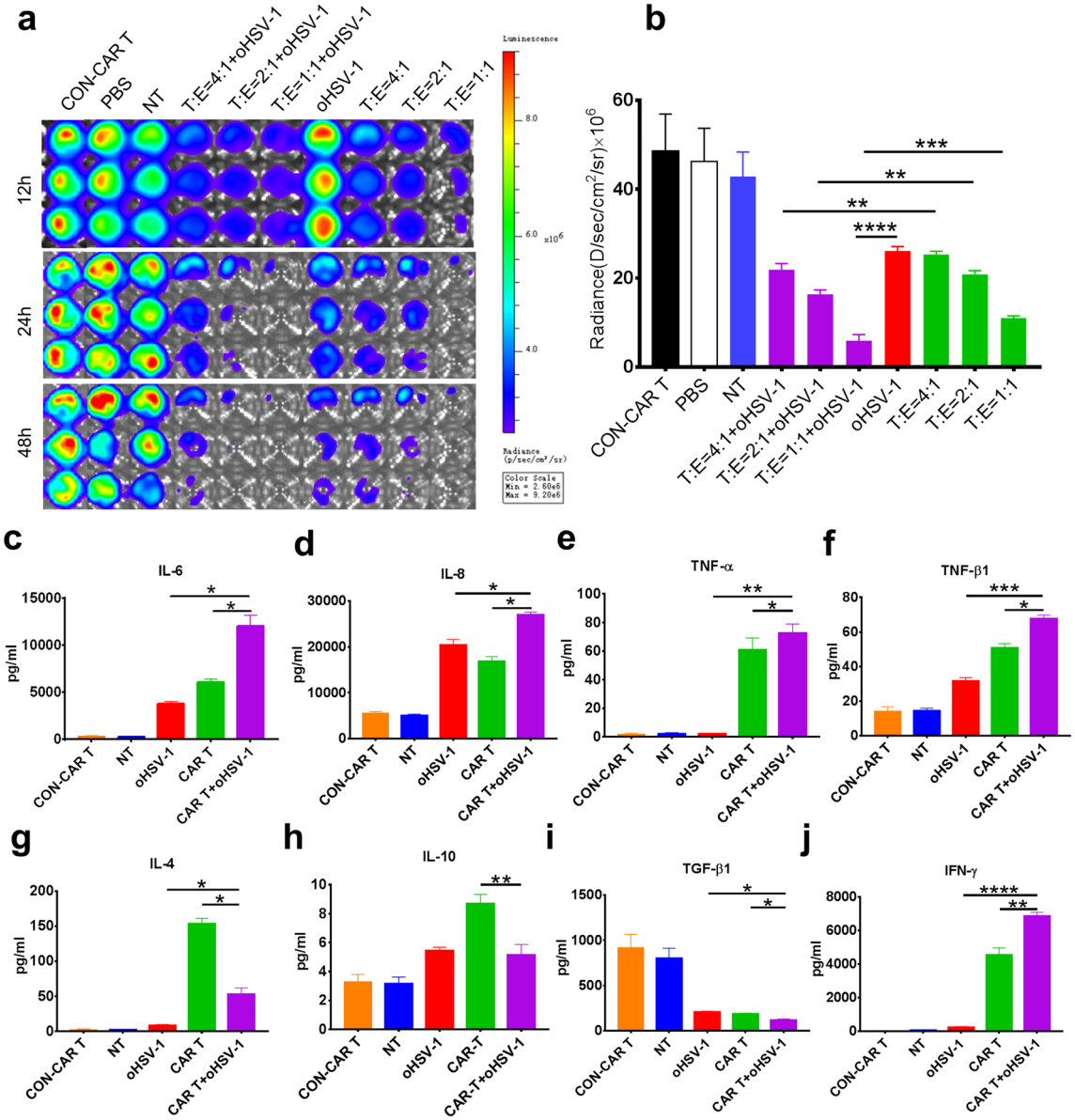

Fig. 2 oHSV-1 combined with CD70 CAR T cells effectively kill GBM cells. **a, b** The killing effects of combinational therapy in GBM cells. U87 are, respectively, cocultured with oHSV-1/CAR T cells or both for 12, 24, 36 h. The IVIS showed combination treatment improves therapeutic efficacy compared with oHSV-1 or CAR T cells alone. The data were representative of 3 experiments from 3 different donors. The data were shown as means ± SD of triplicate wells. *$P<0.05$, ****$P<0.0001$ by 2-way ANOVA with Bonferroni's correction. **c–f** ELISA showed that pro-inflammatory cytokines such as Interleukin I)-6, IL-8, TNF-α, and TNF-β1 are significantly increased during the combined treatment compared with single treatment. The data were shown as means ± SD of triplicate wells. *$P<0.05$, ***$P<0.001$ by 1-way ANOVA with Tukey's post-hoc test. **g–i** ELISA showed that inflammatory inhibitory cytokines such as transforming growth factor (TGF)-β1 IL-10, and IL-4 are decreased. The data were shown as means ± SD of triplicate wells. *$P<0.05$, **$P<0.01$ by 1-way ANOVA with Tukey's post-hoc test. **j** Further examination of IFN-γ, which played an important role in T-cell killing, revealed that the combination treatment group significantly increases interferon (IFN)-γ release. The data were shown as means ± SD of triplicate wells. **$P<0.01$, ****$P<0.0001$ by 1-way ANOVA with Tukey's post-hoc test

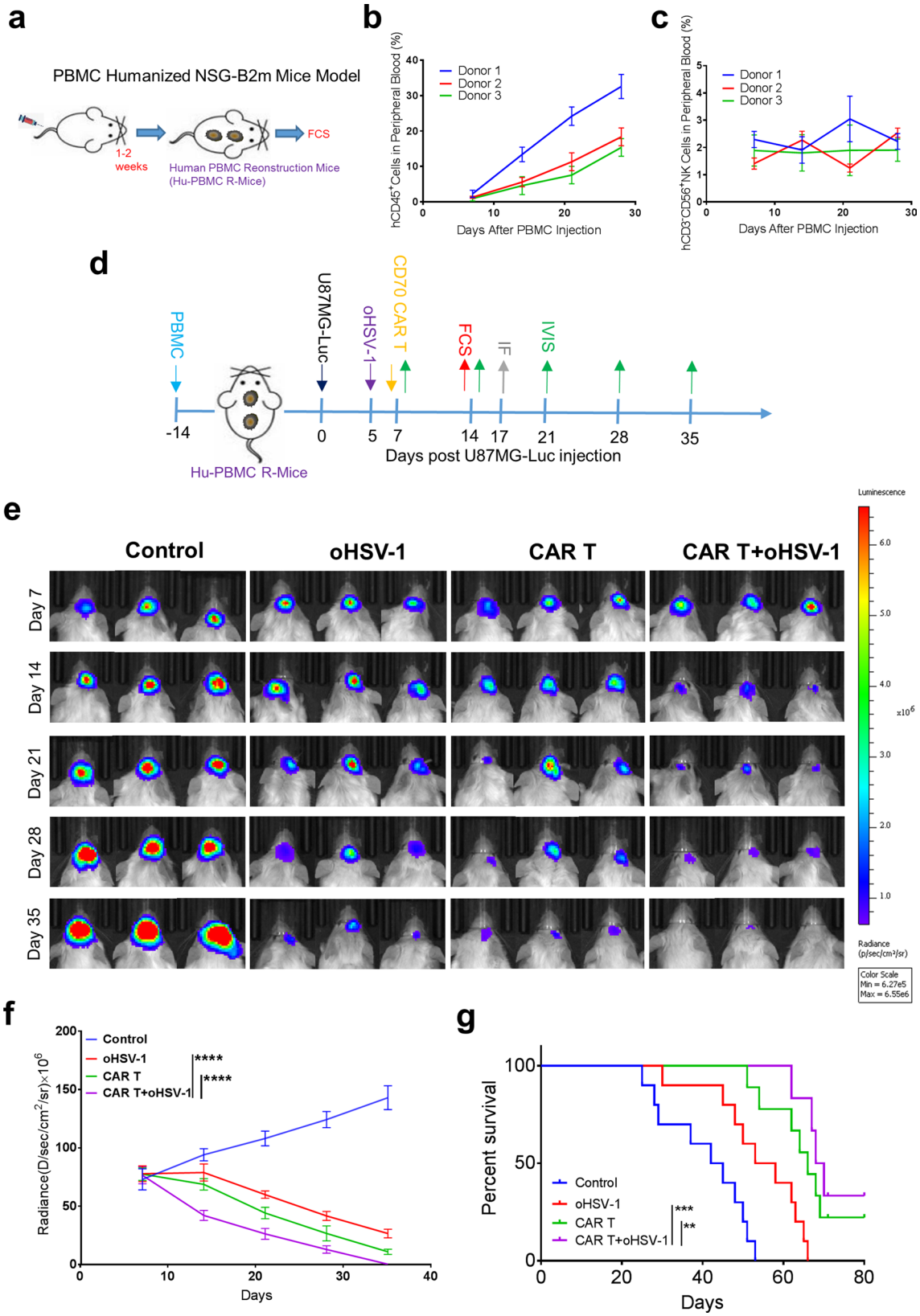
a
PBMC Humanized NSG-B2m Mice Model
1-2 weeks
FCS
Human PBMC Reonstruction Mice (Hu-PBMC R-Mice)
b
hCD45+Cells in Peripheral Blood (%)
Donor 1
Donor 2
Donor 3
Days After PBMC Injection
c
hCD3-CD56+NK Cells in Peripheral Blood (%)
Donor 1
Donor 2
Donor 3
Days After PBMC Injection
d
PBMC
U87MG-Luc
oHSV-1
CD70 CAR T
FCS
IF
IVIS
-14
0
5
7
14
17
21
28
35
Hu-PBMC R-Mice
Days post U87MG-Luc injection
e
Control
oHSV-1
CAR T
CAR T+oHSV-1
Day 7
Day 14
Day 21
Day 28
Day 35
Luminescence
Radiance (p/sec/cm²/sr)
Color Scale Min = 6.27e5 Max = 6.55e6
f
Control
oHSV-1
CAR T
CAR T+oHSV-1
****
****
Radiance(D/sec/cm²/sr)×10⁶
Days
g
Percent survival
Control
oHSV-1
CAR T
CAR T+oHSV-1
***
**
Days

◂**Fig. 3** oHSV-1 combined with CD70 CAR T cells induced tumor regression in the GBM orthotopic xenotransplantation animal model of Peripheral blood mononuclear cell (PBMC) humanized mice. **a** Human PBMCs were injected into NSG-B2m mice via the caudal vein to create PBMC humanized mice. **b, c** The increase in the proportion of $CD45^+$ cells over time was consistent with expectations. Due to the differences in individual donors, the chimera ratio varies. $CD3^-CD56^+$ natural killer (NK) cells were maintained at a low level. The data were representative of 3 experiments from 3 different donors. The data were shown as means ± SD of triplicate wells. **d** To establish the GBM orthotopic xenotransplantation animal model of PBMC humanized mice, GBM was orthotopically injected via a small animal stereotaxic instrument. Five days later, tumor growth was confirmed by IVIS Spectrum, and the combination of oHSV-1 and CD70 CAR T cell therapy was tested in the animal model. **e, f** One week after receiving the combination therapy, significantly better tumor regression was observed compared with single treatment. Thirty-five days after tumor inoculation, most of the mouse tumors receiving combination therapy were disappeared. oHSV-1 or CD70 CAR T-cell monotherapy also reduced tumor growth, and oHSV-1 significantly enhanced the antitumor efficacy of CAR T cells in vivo. The data were shown as means ± SD of triplicate wells. $n = 8$/each group, $^{****}P < 0.0001$ by 2-way ANOVA with Bonferroni's correction. **g** During the observation period of approximately 70 days, 42 ± 6.48% of the mouse tumors disappear in combination therapy, significantly improving the median survival time of the mice. The data were from the experiment shown in figure **F** $^{**}P < 0.01$, $^{***}P < 0.001$ by the log-rank test

end-point (tumor diameter greater than 2 cm) or the end of the experimental period.

Intracranial tumor models and bioluminescence imaging

The PBMCs of the same donor (5×10^6/100 µl) were injected into female 4 to 6-week-old NSG-B2m mice (NOD. Cg-B2mtm1UncPrkdcscid Il2rgtm1Wjl/SzJ; the Jackson Laboratory) via the caudal vein to create PBMC humanized mice. To evaluate the PBMC humanized mouse model, flow cytometry was used to detect the proportion of human $CD45^+$ and $CD3^-CD56^+$ in the peripheral blood of mice every week.

The orthotopic xenotransplantation animal model was constructed as follows. The mice were placed in the prone position on a small animal stereotaxic instrument (David Kopf Instruments, Tujunga, CA, USA) in a barrier environment after PBMC humanized NSG-B2m mice were anesthetized with isoflurane (2% for anesthesia induction and 1% for maintenance) using the Gas Anesthesia System (Perkin-Elmer, Waltham, MA, USA). GBM was inoculated into the right caudate nucleus (coordinates from the bregma: Anterior–Posterior (AP) = 0, Medial–Lateral (ML) = 3, Dorsal–Ventral (DV) = 5.5 mm). After positioning the animal in a stereotactic surgical frame, the stereotactic needle was advanced 3 mm below the dura (advanced needle 3.3 mm and then back 0.3 mm). Tumor cells (10^5/5 µl) were injected into the target area at a rate of 1 µl/minute. The needle was left for 10 min before withdrawal, the injection site was closed with bone wax, and the scalp was sutured. GBM was inoculated into the right caudate nucleus. Tumor cells (10^5/5 µl) were injected into the target area at a rate of 1 µl/minute. The mice were kept and observed until recovery from the anesthesia.

On the 5th day after tumor inoculation, in vivo bioluminescence imaging was performed 5 min after intraperitoneal injection of 3 mg of D-luciferin (Promega, Madison, WI, USA) in phosphate buffer saline (PBS) (100 µl) with IVIS Spectrum. IVIS monitored the intracranial tumor changes weekly. oHSV-1 (1×10^6 pfu/5 µl) or PBS (control) was injected intratumorally in the same stereotactic orientation. On day 7, CD70 CAR T cells (10^6/100 µl) or NT cells was injected via the caudal vein. Each group comprised 8 mice, and all the experiments were repeated at least twice in a blinded and randomized fashion. At the same time, the survival days of the mice were recorded for survival analysis. All the experiments were carried out randomly and blindly.

Flow cytometry

To evaluate the transduction efficiency and number of T cells, flow cytometry analysis was performed using fluorochrome-conjugated antibodies. The single-cell suspensions were incubated in the dark at 4 °C for 30 min with human CD3 Mouse mAb-PerCP/Cy5.5 (StemCell Technologies, Vancouver, BC, Canada). Next, the cells were centrifuged, resuspended in PBS and analyzed using a flow cytometer (BD biosciences, San Jose, CA, USA). The data were collected and analyzed using FlowJo software (TreeStar, Ashland, OR, USA).

One week after the combined treatment, the mice were euthanized under anesthesia. The brain tumor tissue of the mice was mechanically cut into pieces, passed through a 70 µm filter twice and washed with D-phosphate-buffered saline. Single-cell suspensions were treated with the following antibodies: CD3-PerCP/Cy5.5, APC-Cy7 anti-human CD4 (4A Biotech Co., Ltd, Beijing, China), PE anti-human CD8 (4A Biotech Co., Ltd, Beijing, China), APC anti-human IFN-γ (4A Biotech Co., Ltd, Beijing, China), APC anti-human CD56 (4A Biotech Co., Ltd, Beijing, China), PE anti-human Foxp3 (4A Biotech Co., Ltd, Beijing, China), and APC anti-human CD25 (4A Biotech Co., Ltd, Beijing, China). Harvested cells were incubated with Human BD Fc Block TM (BD Biosciences, San Jose, CA, USA) to block fc receptors. To detect T cells expressing IFN-γ in brain tumor tissues, the cells were resuspended in DMEM containing Cell Stimulation Cocktail (4A Biotech Co., Ltd, Beijing, China) and incubated for 4 h. The harvested cells were stained with cell surface antibody CD3-PerCP/Cy5.5 and APC-Cy7 anti-human CD4. Thereafter, the permeabilized cells were stained with intracellular cytokines

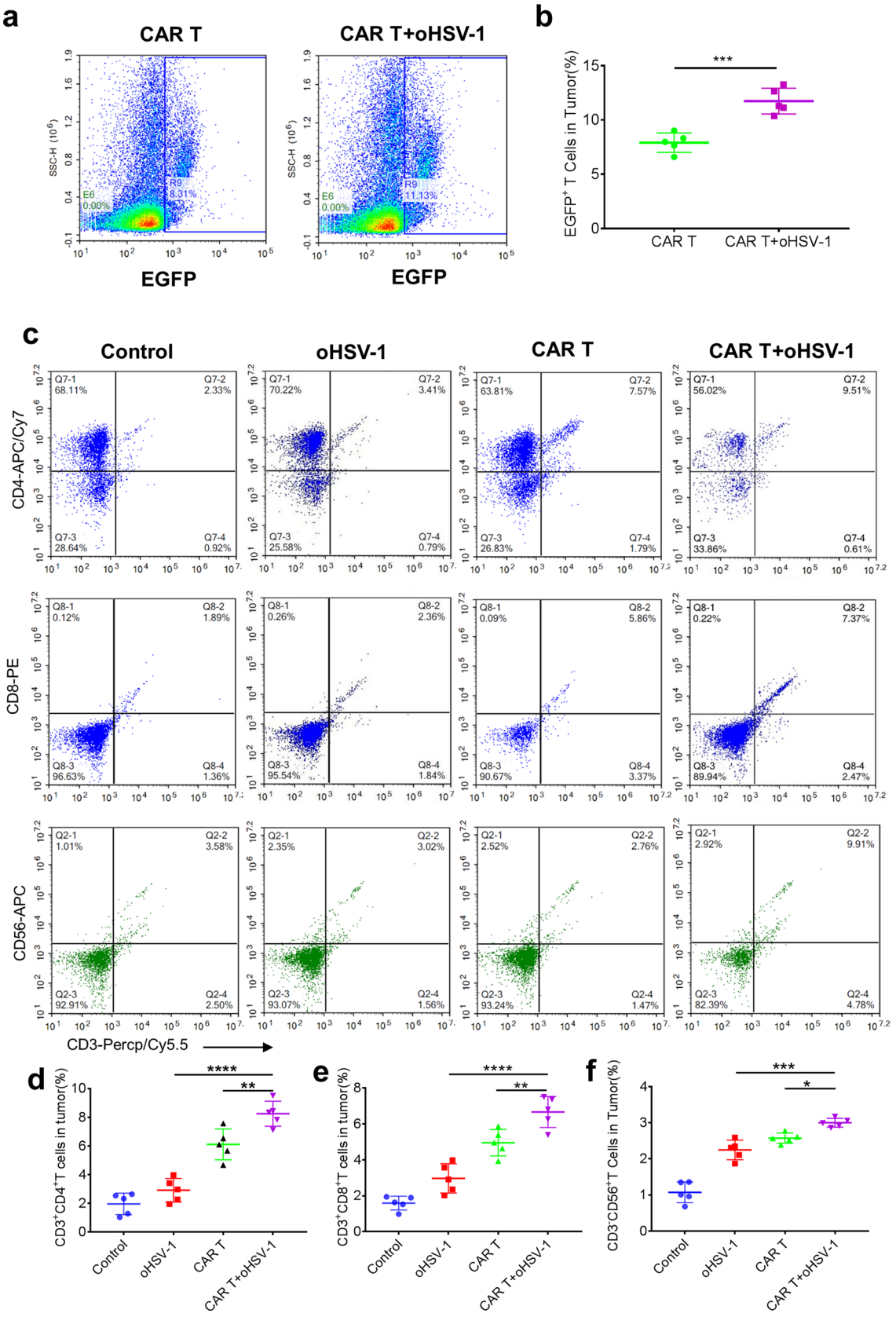
a
CAR T
CAR T+oHSV-1
SSC-H (10^6)
EGFP
R9
8.31%
11.13%
E6
0.00%
b
EGFP+ T Cells in Tumor(%)
***
CAR T
CAR T+oHSV-1
c
Control
oHSV-1
CAR T
CAR T+oHSV-1
CD4-APC/Cy7
CD8-PE
CD56-APC
CD3-Percp/Cy5.5
Q7-1 68.11%
Q7-2 2.33%
Q7-3 28.64%
Q7-4 0.92%
Q7-1 70.22%
Q7-2 3.41%
Q7-3 25.58%
Q7-4 0.79%
Q7-1 63.81%
Q7-2 7.57%
Q7-3 26.83%
Q7-4 1.79%
Q7-1 56.02%
Q7-2 9.51%
Q7-3 33.86%
Q7-4 0.61%
Q8-1 0.12%
Q8-2 1.89%
Q8-3 96.63%
Q8-4 1.36%
Q8-1 0.26%
Q8-2 2.36%
Q8-3 95.54%
Q8-4 1.84%
Q8-1 0.09%
Q8-2 5.86%
Q8-3 90.67%
Q8-4 3.37%
Q8-1 0.22%
Q8-2 7.37%
Q8-3 89.94%
Q8-4 2.47%
Q2-1 1.01%
Q2-2 3.58%
Q2-3 92.91%
Q2-4 2.50%
Q2-1 2.35%
Q2-2 3.02%
Q2-3 93.07%
Q2-4 1.56%
Q2-1 2.52%
Q2-2 2.76%
Q2-3 93.24%
Q2-4 1.47%
Q2-1 2.92%
Q2-2 9.91%
Q2-3 82.39%
Q2-4 4.78%
d
CD3+CD4+T cells in tumor(%)
****
**
e
CD3+CD8+T cells in tumor(%)
****
**
f
CD3-CD56+T Cells in Tumor(%)
***
*
Control
oHSV-1
CAR T
CAR T+oHSV-1

◂**Fig. 4** oHSV-1 and CD70 CAR T cell combination therapy increased the proportion of T cells and NK cells in theTME. **a, b** To determine whether oHSV-1 could improve CAR T-cell infiltration into tumors, we used flow cytometry to detect $EGFP^+$CAR T cells in tumor tissues. The CAR T-cell treatment group alone showed low levels of implantation. By contrast, oHSV-1 infection induced higher accumulation of $EGFP^+$CAR T cells. The data were shown as means ± SD of triplicate wells. ****P < 0.001* by 1-way ANOVA with Tukey's post-hoc test. **c–e** Flow cytometry data analysis showed that, compared with oHSV-1 or CD70 CAR T-cell monotherapy, $CD4^+$ and $CD8^+$ T-cell infiltration in the TME with the combined treatment of oHSV-1 and CD70 CAR T cells was increased. The data were shown as means ± SD of triplicate wells. ***P < 0.01, ****P < 0.0001* by 1-way ANOVA with Tukey's post-hoc test. **f** Excitingly, although PBMC humanized mice only reconstructed low levels of human NK cells, flow cytometry data analysis showed increased $CD3^-CD56^+$ NK cell infiltration with the combined treatment. The data were shown as means ± SD of triplicate wells. *P < 0.05, ***P < 0.001* by 1-way ANOVA with Tukey's post-hoc test

using anti-IFN-γ mAb. To determine the percentage of $CD4^+CD25^+Foxp3^+$ regulatory T (Treg) cells, the harvested cells were stained with APC-Cy7 anti-human CD4, APC anti-human CD25, and PE anti-human Foxp3 according to the manufacturer's protocols. The antibodies used to identify natural killer (NK) cells were as follows: CD3-PerCP/Cy5.5 and APC anti-human CD56. The isotype negative control antibody was the human IgG isotype. Flow cytometry analysis was performed using an ACEA Novocyte flow cytometer (ACEA Biosciences Inc., San Diego, CA, USA). The data were analyzed using ACEA NovoExpress™ software.

Immunofluorescence

IF was performed on paraformaldehyde-fixed, paraffin-embedded sections. To prepare paraffin sections of the tumor, whole-body perfusion was carried out using PBS followed by 4% paraformaldehyde. A paraffin slicing machine (Leica, Wetzlar, Germany) was used to make tumor tissue Sections (5 μm). Standard staining immunofluorescence protocols were followed. The primary antibodies were as follows: anti-human CD8 (Thermo Fisher Scientific, Waltham, MA, USA), anti-human CD56 (Thermo Fisher Scientific, Waltham, MA, USA), and anti-human TGF-β1 (Abcam, Cambridge, MA, USA). The secondary antibodies used were FITC anti-mouse and Cy3 anti-rabbit (Jackson Immunoresearch, West Grove, PA, USA). Immunofluorescence-stained tissue slides were scanned using a ScanScope XT slide scanner (Aperio Technologies, CA, USA). Images were analyzed using Aperio ImageScope software (Leica Biosystems, Buffalo Grove, IL, USA).

Statistics

Statistical analyses were performed using GraphPad Prism 7.0. Unless specifically noted, all the data were representative of at least three separate experiments. Error bars represented the standard deviation (SD) and were calculated using Prism. The specific statistical tests used were t test for single comparisons and ANOVA followed by Tukey's test for multiple comparisons. Repeated-measures 2-way ANOVA with Bonferroni's correction was used to compare the effect of multiple levels of 2 factors with multiple observations at each level. GraphPad Prism was used to compare different group survival curves with the log-rank test. All P values < 0.05 were considered statistically significant.

Results

CD70 CAR T cells specifically recognized GBM

Human T cells were successfully isolated from fresh peripheral blood from healthy donors. Flow cytometry analysis revealed that 98% of the cells highly expressed CD3 (Fig. 1b). Prior evidence showed that CD70 is naturally expressed in GBM cells [22]. To investigate whether CD70 could be used as a target for immunotherapy, we constructed human CD70 CAR T (Lv-trCD27-2ndCAR T) cells. To detect the expression of enhanced green fluorescent protein (EGFP) by flow cytometry, we obtained CD70 CAR T cells with a positive rate of 46% (Fig. 1b).

After coculture of CD70 CAR T cells and GBM, mouse Anti-Human CD70 immunofluorescence staining showed that $EGFP^+$CAR T cells specifically recognized $CD70^+$GBM (Fig. 1c). These tumor cells are being recognized and attacked by CD70 CAR T cells not Con-CAR T cells, which photographed by fluorescence microscope. SEM showed that CAR T cells engulfed tumor cells. After the CAR T cells approach and recognize the tumor cells, they gather toward the tumor cells and approach each other, and then stretch out pseudopods to capture the tumor cells. (Fig. 1d).

Secretion of factors in conditioned media

To determine secretion of cytokines in different conditioned media, we used Luminex assay to detect various cytokines in conditioned media. The secretion from oHSV-1-infected GBM is shown in Fig. 1e. Moreover, ELISA showed that the expression levels of pro-inflammatory cytokines such as IL-6, IL-8, TNF-α, and TNF-β1 were significantly increased during the combined treatment compared with single treatment (Fig. 2c–f). In contrast, the levels of inflammatory inhibitory cytokines such as TGF-β1, IL-10, and IL-4 were decreased (Fig. 2g–i). Identically, IFN-γ release in combination treatment group was significantly increased compared to alone treatment (Fig. 2j). To further study the time secretion

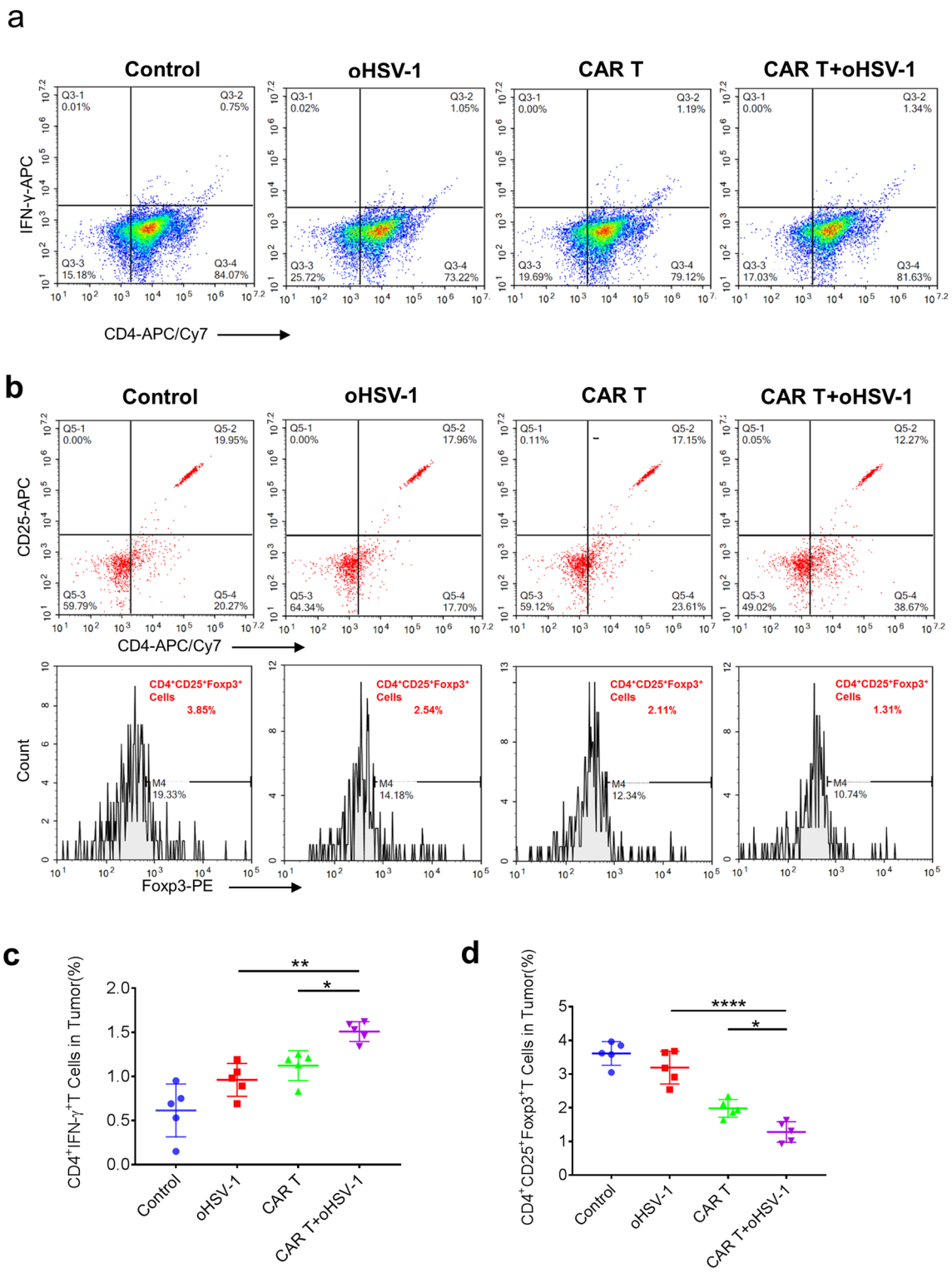

Fig. 5 Combination of oHSV-1 and CD70 CAR T cells increased the proportion of $CD4^+IFN\text{-}\gamma^+$ T cells and reduces the proportion of Treg cells in GBM model. **a** Flow cytometry detected the percentage of $CD4^+IFN\text{-}\gamma^+$ T cells in tumors after the combination treatment. The proportion of $CD4^+IFN\text{-}\gamma^+$ in combinational therapy was increased compared to control group. **b** The effects of dual combination on Treg cells in GBM tumors. The detection of $CD4^+CD25^+Foxp3^+$ Treg cells by flow cytometry showed that combination treatment could reduce the proportion of $CD4^+CD25^+Foxp3^+$ Treg cells in tumors. **c** Quantification of $CD4^+$ IFN-γ^+ T cells in tumors. **d** Quantification of $CD4^+CD25^+Foxp3^+$ Treg cells in tumors. The data were shown as means ± SD of triplicate wells. $*P<0.05$, $****P<0.0001$ by 1-way ANOVA with Tukey's post-hoc test

of IFN-γ, ELISA was performed to examine the levels of supernatants from oHSV-1-infected GBM at different time point. We found that interferon secretion increased gradually and reached a peak at 48 h (Fig. 1f).

oHSV-1 combined with CD70 CAR T cells contributed to improve therapeutic efficacy

We first infected and killed the tumor cells as described previously [24, 25]. Combination therapy killed most of the tumor cells within 24 h and almost all the tumor cells within 48 h when the effector/target ratio was 1:1 (Fig. 2a, b). Compared with oHSV-1 or CD70 CAR T cells alone, combined oHSV-1 and CD70 CAR T cells led to faster lysis of GBM cells. This finding was consistent with the result that oHSV-1 preinfection increased the activity of T cells.

Dual combination of oHSV-1 and CD70 CAR T cells achieved optimum anticancer benefit in mouse GBM

Human PBMCs were injected into NSG-B2m mice via the caudal vein to create PBMC humanized mice (Fig. 3a). The increase in the proportion of $CD45^+$ cells over time was consistent with expectations. Due to the differences in individual donors, the chimera ratio varied (Fig. 3b). $CD3^-CD56^+$ NK cells maintained a low level (Fig. 3c). Thus, PBMC humanized NSG-B2m mice mainly comprising T cells, and a small amount of NK cells were successfully established.

Additionally, we tested the combination of oHSV-1 and CD70 CAR T-cell therapy in animal model and found the dual combination significantly enhanced anti-GBM efficacy compared to single treatment (Fig. 3d–f). During the observation period of approximately 70 days, $42 \pm 6.48\%$ of the mouse tumors disappeared in combination therapy; in particular, combination therapy significantly improved the median survival time of the mice (Fig. 3g).

Effect of dual combination treatment on tumor-associated immune cells

The animals were treated according to the procedure in Fig. 3D. And then we used flow cytometry to detect $EGFP^+$CAR T cells in tumor tissues. The CAR T-cell treatment group alone showed low levels of implantation. By contrast, oHSV-1 infection induced higher accumulation of $EGFP^+$CAR T cells (Fig. 4a, b). Flow cytometry data analysis showed that the infiltration of $CD4^+$ and $CD8^+$ T cells in the TME of the combined treatment was increased at day 14 (Fig. 4c–e). In particular, the proportion of $CD4^+$ IFN-γ^+ T cells in the combination therapy group was increased (Fig. 5a, c). IF analysis also showed that the tumors in the combination treatment group were significantly infiltrated with $CD8^+$ T cells (Fig. 6a), reduced the expression of immunosuppressive TGF-β1 in tumor tissues, and promoted infiltration NK cells (Fig. 6b).

Flow cytometry data analysis and IF images showed an increase in $CD3^-CD56^+$ NK cell infiltration in the combined treatment, further increasing the killing effect on the tumor (Fig. 4c, f; 6b). The detection of $CD4^+CD25^+Foxp3^+$ Treg cells by flow cytometry showed that combination therapy reduced the proportion of $CD4^+CD25^+Foxp^{3+}$ Treg cells in tumors (Fig. 5b, d).

Discussion

The immunotherapy represented by CAR T provides a particularly promising strategy for the treatment of intracranial tumors [27]. However, gliomas are considered “cold” in immunology, and CAR T cells cannot circumvent the poor infiltration of T cells when used to treat solid tumors. The transport, proliferation, and long-term infiltration of specific T cells in tumor tissues are crucial to effective antitumor activity [28, 29]. The central nervous system has a unique immune microenvironment. Immune surveillance in the central nervous system is much more complicated [30]. OVs can modulate immunity and participate in the inherent advantages of immunotherapy [5], effectively helping the efficacy of CAR T-cell therapy and providing various promising combinations. However, the relative contribution of these mechanisms depends on the complex interaction between different factors, such as viral vectors, CAR T-cell targets, cancer cell types, and host immunity [31]. Therefore, each combination needs to be optimized independently to achieve the best synergy between these two treatment modalities. Choosing the right OVs, timing of infection, and target of combined CAR T cells are vital to improve the efficacy of combined therapy. The schematic diagram of dual combination treatment is shown in Fig. 7.

oHSV-1 infection of tumor cells can transform malignant tumor cells into cytokine and chemokine factories, thereby transforming the TME from immunosuppression to an immune stimulation environment that allows T-cell entry and activation. This potential creates opportunities for synergy with CAR T-cell immunotherapy. oHSV-1 can induce enhanced effects of type I IFN in the TME. Type I IFN promotes $CD8^+$ T-cell proliferation, effector function, and immune memory formation by stimulating the host's adaptive immune system [32]. IFN-β can inhibit the activation and proliferation of Treg cells and destroy tumor microvessels [33]. Through this effect, the tumor's "cold" immune microenvironment is transformed into "hot", thereby increasing the infiltration of CAR T cells [34]. GBM cells preinfected with oHSV-1 significantly increased the proliferation and activity of T cells during coculture with CD70 CAR T cells. We found that pro-inflammatory

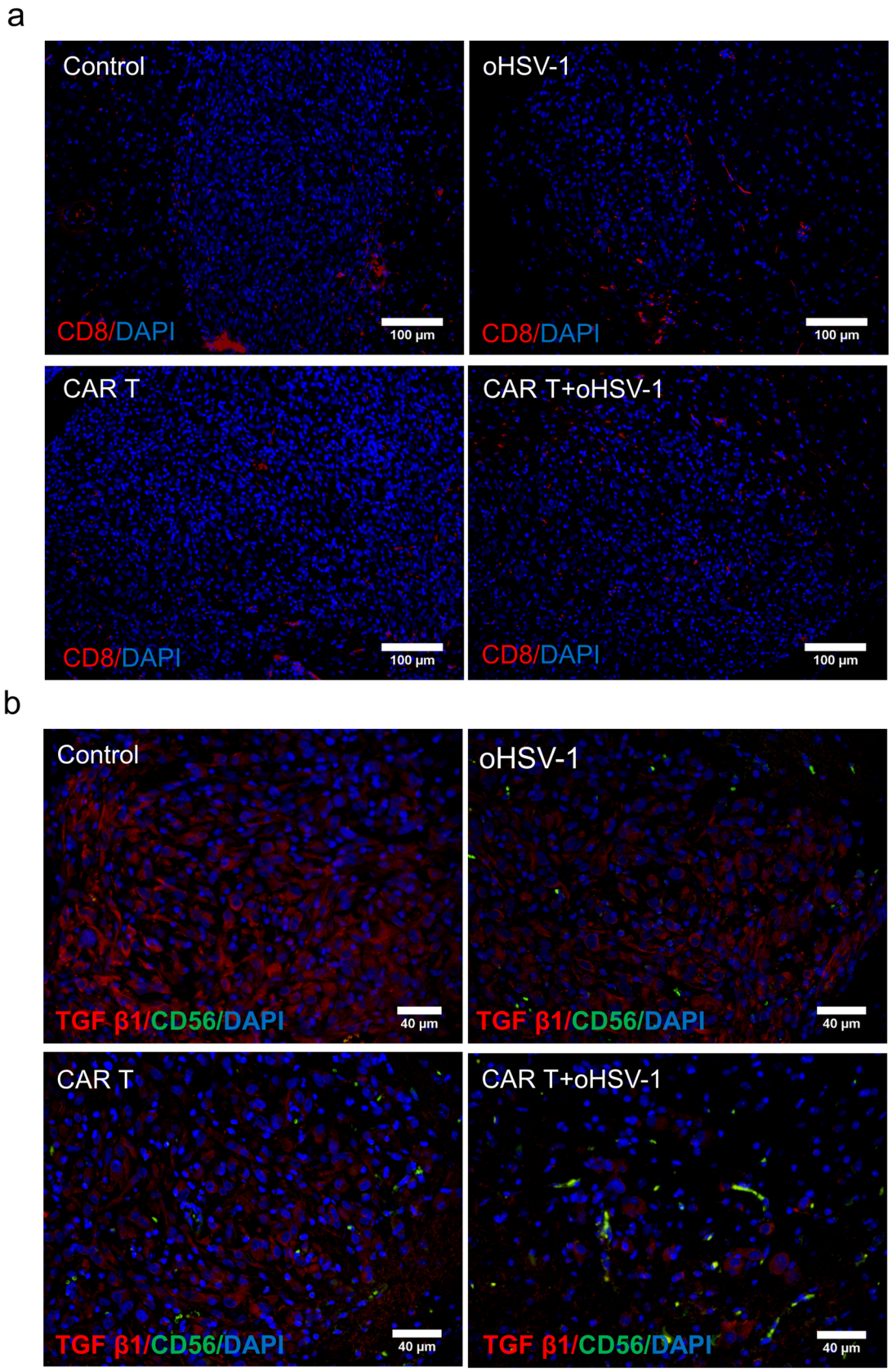
a
Control
CD8/DAPI
100 μm
oHSV-1
CD8/DAPI
100 μm
CAR T
CD8/DAPI
100 μm
CAR T+oHSV-1
CD8/DAPI
100 μm
b
Control
TGF β1/CD56/DAPI
40 μm
oHSV-1
TGF β1/CD56/DAPI
40 μm
CAR T
TGF β1/CD56/DAPI
40 μm
CAR T+oHSV-1
TGF β1/CD56/DAPI
40 μm

◂**Fig. 6** oHSV-1 and CD70 CAR T-cell combination therapy increased $CD8^+$ T cell and NK cell infiltration and reduced TGF-β1 expression. **a** Immunofluorescence analysis showed that the tumors in the combination treatment group were significantly infiltrated with $CD8^+$ T cells, while the control group showed only low-level infiltration of tumor-related boundaries on day 17. IF images were analyzed using the Aperio ImageScope software. Red, $CD8^+$ T cells; Blue, 2-(4-Amidinophenyl)-6-indolecarbamidine dihydrochloride (DAPI). Original magnification, ×20. Scale bars: 100 μm. **b** Combination therapy significantly reduced the expression of immunosuppressive TGF-β1 in tumor tissues, forming a pro-inflammatory immune microenvironment and promoting the infiltration of NK cells. IF images were analyzed using the Aperio ImageScope software. Green, $CD56^+$ NK cells; Red, TGF-$β1^+$ cells; Blue, DAPI. Original magnification, ×40. Scale bars: 40 μm

cytokines, such asIL-6, IL-8, TNF-α, and TNF-β1 were significantly increased, while the anti-inflammatory factors TGF-β1, IL-10, and IL-4 were decreased, suggesting potential antitumor efficacy. TNF-α and other primary pro-inflammatory mediators can induce T-cell-attracting chemokine [35]. Chemokines are secondary pro-inflammatory mediators that play important roles in the recruitment of immune cells [36]. We found that combination treatment significantly increased the release of IFN-γ. These results indicate that oHSV-1, CAR T, and GBM interact with each other in the coculture system to form a pro-inflammatory local environment. In particular, through the study of tumor-bearing PBMC humanized NSG-B2m mice, we found that combination therapy can significantly reduce the expression of immunosuppressive TGF-β1 in tumor tissues, forming a pro-inflammatory immune microenvironment.

oHSV-1 affects the TME by modulating immune cells [37, 38] and triggers the expression of tumor-associated antigens [39]. Infiltrating T cells in the TME circulate to kill tumor cells expressing specific antigen. Moreover, due to the cytotoxic perforation and the local release of telomerase cause immune-related "bystander effects", which can kill tumor cells that do not express direct antigens near the tumor cells [40]. Theoretically, CAR T cells in the peripheral blood of mice will undergo a proliferation process. This is based on CAR T derived from the PBMC of the same volunteer. The PBMC of this volunteer is also used to construct humanized immune system mice. Our results showed that CAR T cells in the combined treatment group only slightly proliferated, probably because of local injection of the virus, lead to small impact on the systemic immune system (Supplemental figure). Moreover, the intratumoral injection of the virus mainly changes the local tumor microenvironment and indirectly increases the infiltration of CAR T cells to achieve complementary curative effects. In the present study, the GBM orthotopic xenotransplanted PBMC humanized mouse model responded quickly to combination therapy. Once OVs infects malignant tumor cells, they initiate an antiviral response, resulting in the production and release of reactive oxygen species and antiviral cytokines. This excellent combination therapy can increase the infiltration of T cells and NK cells in the tumor, while reducing the number of immunosuppressed Treg cells and TGF-β1 expression in the tumor. In a complex immunosuppressive TME, the function of T cells is inhibited by different immune cells and cytokines through multiple pathways. Studies have shown that TGF-β1 can induce CAR T-cell failure, and inhibition of TGF-β1 expression can enhance the function of CAR T cells in the TME [16]. Our study showed that combination therapy inhibits the expression of TGF-β1, which also promotes the formation of a pro-inflammatory environment. Although the understanding of the TME remains limited and incomplete [28], we have also revealed various immune cells in the TME simulated by the humanized immune system in combination immunotherapy. These findings provide insights into the development and utilization of immunotherapy to target the TME to treat glioma.

The lack of animal models restricts the effect of OVs on CAR T-cell therapy [41]. Xenograft NSG-B2m mice of human-derived glioma cell lines are useful tools to evaluate the antitumor efficacy of CAR T cells. However, due to severe defects in the immune system of NSG mice, it cannot cooperate with the implantation of human-derived glioma cell lines to form a complete immunosuppressive TME [42]. These tumor xenografts cannot assess the ability of OVs to induce antitumor immunity [41]. Although CAR T cells targeting tumor-associated antigen are a prospective therapeutic strategy for GBM [43], the outcome remains limited. The biological properties of mouse-derived glioma cell lines are different from those of human-derived glioma cell lines. We established animal models that tolerate human-derived glioma cells and realistically simulated the GBM microenvironment, and the application of humanized immune system mice has become increasingly widespread. To delay the occurrence of graft versus host disease, provide a longer observation period and simulate a relatively ideal immune environment, human PBMCs were injected into NSG-B2m mice via the caudal vein to create PBMC humanized mice. PBMC humanized NSG-B2m mice mainly comprising T cells and containing a small amount of NK cells were successfully established. Although partial reconstruction of the human-derived immune system was obtained that cannot ideally reproduce the immunosuppressed tumor microenvironment, it also provided new methods and ideas to study the immunomodulatory effects of OVs and CAR T-cell therapy.

Conclusions

In summary, these results indicated that oHSV-1 could enhance the therapeutic efficacy of CD70 CAR T cells. The dual combination was reasonable and excellent, and together

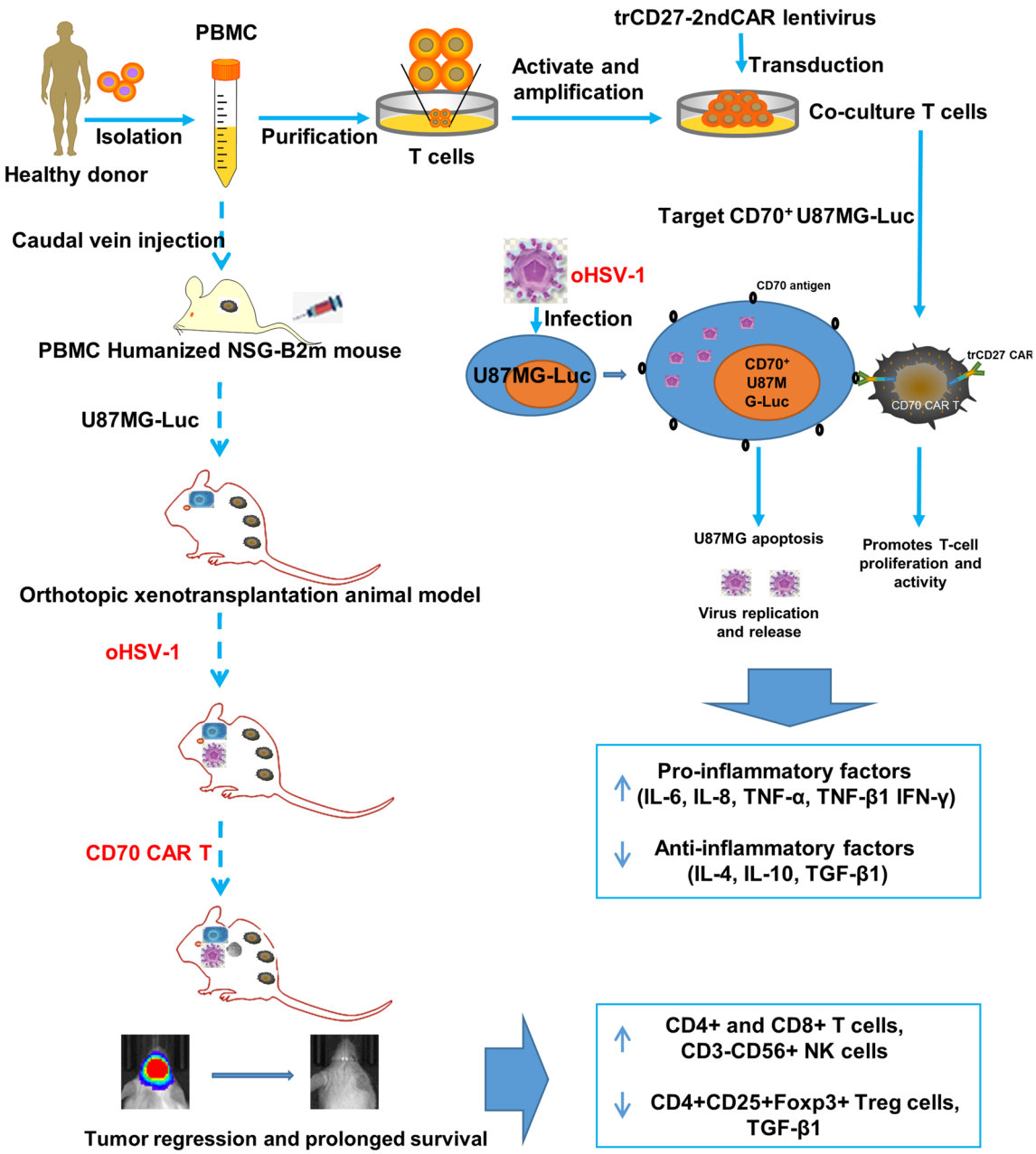

Fig. 7 Schematic diagram displaying the important role of oHSV-1 and CD70 CAR T cells in the treatment of GBM. Based on the findings of the present study, oHSV-1 could enhance the therapeutic efficacy of CD70 CAR T cells. The dual combination was reasonable and excellent, and together transformed the immunosuppressed TME into a pro-inflammatory immune environment

transformed the immunosuppressed TME into a pro-inflammatory immune environment. Through our joint efforts to explore potential, novel and promising immunotherapeutic strategies that could target TME, we could bring hope to glioma patients with this new perspective for the combined immunotherapy of glioma patients.

Supplementary Information The online version contains supplementary material available at https://doi.org/10.1007/s00262-022-03172-x.

Author contributions F.S.L and G.D.Z were responsible for design of the experiments, G.D.Z., J.W.Z and Q.Z performed the experiments, Q.Z., J.W.Z., F.S.L and G.S. J were responsible for acquisition of the data, G.D.Z., Q.Z. and X.D.S analyzed the data and prepared the manuscript, G.D.Z., J.W.Z., Q.Z., G.S.J., X.D.S. and F.S.L wrote the manuscript. All authors have read and approved the final version.

Funding This work was supported by grants from the Beijing Natural Science Foundation Program and Scientific Research Key Program of the Beijing Municipal Commission of Education (KZ202010025034),

the Capital's Funds for Health Improvement and Research (CFH, 2020–1-1071), the National Natural Science Foundation of China (No, 81672478), the Natural Science Foundation of Beijing Municipality (No. 7202020) and the Beijing Laboratory of Biomedical Materials Foundation.

Availability of data and materials All data generated in this study are available from the corresponding author on reasonable request.

Declarations

Conflict of interest The authors declare no conflicts of interest.

Ethics approval and consent to participate The Experimental Animal Welfare and Ethics Committee of Beijing Tiantan Hospital affiliated to Capital Medical University and approved all the animal experiments. The use of tissue samples from patients with glioblastoma and the peripheral blood of healthy donors were approved by Ethics Committee of Beijing Tiantan Hospital affiliated to Capital Medical University.

Consent for publication Not applicable. All authors read and approved the manuscript.

References

1. Migliorini D, Dietrich P Y, Stupp R, Linette G P, Posey A D, Jr., June C H (2018) CAR T-Cell therapies in glioblastoma: a first look. Clin Cancer Res. 24: 535-540.
2. Seystahl K, Wick W, Weller M (2016) Therapeutic options in recurrent glioblastoma–an update. Crit Rev Oncol Hematol 99:389–408
3. Zhang Q, Liu F (2020) Advances and potential pitfalls of oncolytic viruses expressing immunomodulatory transgene therapy for malignant gliomas. Cell Death Dis 11:485
4. Lichty BD, Breitbach CJ, Stojdl DF, Bell JC (2014) Going viral with cancer immunotherapy. Nat Rev Cancer 14:559–567
5. Kaufman HL, Kohlhapp FJ, Zloza A (2016) Oncolytic viruses: a new class of immunotherapy drugs. Nat Rev Drug Discov 15:660
6. Twumasiboateng K, Pettigrew JL, Kwok YYE, Bell JC, Nelson BH (2018) Oncolytic viruses as engineering platforms for combination immunotherapy. Nat Rev Cancer 18:419–432
7. Marelli G, Howells A, Lemoine NR, Wang Y (2018) Oncolytic viral therapy and the immune system: a double-edged sword against cancer. Front Immunol 9:866
8. Bommareddy PK, Shettigar M, Kaufman HL (2018) Integrating oncolytic viruses in combination cancer immunotherapy. Nat Rev Immunol 18:498–513
9. Grupp SA, Kalos M, Barrett D, Aplenc R, Porter DL, Rheingold SR et al (2013) Chimeric antigen receptor-modified T cells for acute lymphoid leukemia. N Engl J Med 368:1509–1518
10. O'Rourke D M, Nasrallah M P, Desai A, Melenhorst J J, Mansfield K, Morrissette J J D, et al. (2017) A single dose of peripherally infused EGFRvIII-directed CAR T cells mediates antigen loss and induces adaptive resistance in patients with recurrent glioblastoma. Sci Transl Med. 9
11. Liyanage UK, Moore TT, Joo HG, Tanaka Y, Herrmann V, Doherty G et al (2002) Prevalence of regulatory T cells is increased in peripheral blood and tumor microenvironment of patients with pancreas or breast adenocarcinoma. J Immunol 169:2756–2761
12. Mukherjee P, Ginardi AR, Madsen CS, Tinder TL, Jacobs F, Parker J et al (2001) MUC1-specific CTLs are non-functional within a pancreatic tumor microenvironment. Glycoconj J 18:931–942
13. Moon EK, Wang L, Dolfi DV, Wilson CB, Ranganathan R, Sun J et al (2014) Multifactorial T-cell hypofunction that is reversible can limit the efficacy of chimeric antigen receptor-transduced human T cells in solid tumors. Clin Cancer Res 20:4262–4273
14. Beatty GL, Ohara MH (2016) Chimeric antigen receptor-modified T cells for the treatment of solid tumors: defining the challenges and next steps. Pharmacol Ther 166:30–39
15. Newick K, Moon EK, Albelda SM (2016) Chimeric antigen receptor T-cell therapy for solid tumors. Mole Ther–Oncolytics 3:16006–16006
16. Tang N, Cheng C, Zhang X, Qiao M, Li N, Mu W, et al. (2020) TGF-beta inhibition via CRISPR promotes the long-term efficacy of CAR T cells against solid tumors. JCI Insight. 5:
17. Teng R, Zhao J, Zhao Y, Gao J, Li H, Zhou S et al (2019) Chimeric antigen receptor-modified T cells repressed solid tumors and their relapse in an established patient-derived colon carcinoma xenograft model. J Immunother 42:33–42
18. Ma S, Li X, Wang X, Cheng L, Li Z, Zhang C et al (2019) Current progress in CAR-T cell therapy for solid tumors. Int J Biol Sci 15:2548–2560
19. Ma L, Dichwalkar TM, Chang JY, Cossette B, Garafola D, Zhang AQ et al (2019) Enhanced CAR-T cell activity against solid tumors by vaccine boosting through the chimeric receptor. Science 365:162–168
20. Yamamoto TN, Kishton RJ, Restifo NP (2019) Developing neoantigen-targeted T cell–based treatments for solid tumors. Nat Med 25:1488–1499
21. Hintzen RQ, Lens SMA, Beckmann MP, Goodwin RG, Lynch DH, Van Lier RAW (1994) Characterization of the human CD27 ligand, a novel member of the TNF gene family. J Immunol 152:1762–1773
22. Jin L, Ge H, Long Y, Yang C, Chang Y, Mu L et al (2018) CD70, a novel target of CAR T-cell therapy for gliomas. Neuro Oncol 20:55–65
23. De Meulenaere A, Vermassen T, Aspeslagh S, Zwaenepoel K, Deron P, Duprez F et al (2016) CD70 expression and its correlation with clinicopathological variables in squamous cell carcinoma of the head and neck. Pathobiology 83:327–333
24. Zhang G, Jin G, Nie X, Mi R, Zhu G, Jia W et al (2014) Enhanced antitumor efficacy of an oncolytic herpes simplex virus expressing an endostatin-angiostatin fusion gene in human glioblastoma stem cell xenografts. PLoS ONE 9:e95872
25. Zhu G, Su W, Jin G, Xu F, Hao S, Guan F et al (2011) Glioma stem cells targeted by oncolytic virus carrying endostatin-angiostatin fusion gene and the expression of its exogenous gene in vitro. Brain Res 1390:59–69
26. Wang QJ, Yu Z, Hanada KI, Patel K, Kleiner D, Restifo NP et al (2017) Preclinical evaluation of chimeric antigen receptors targeting CD70-expressing cancers. Clin Cancer Res 23:2267–2276
27. Galea I, Bernardes-Silva M, Forse PA, van Rooijen N, Liblau RS, Perry VH (2007) An antigen-specific pathway for CD8 T cells across the blood-brain barrier. J Exp Med 204:2023–2030
28. Klemm F, Maas R R, Bowman R L, Kornete M, Soukup K, Nassiri S, et al. (2020) Interrogation of the microenvironmental landscape in brain tumors reveals disease-specific alterations of immune cells. Cell. 181: 1643–1660 e1617.
29. Fraietta JA, Lacey SF, Orlando EJ, Pruteanu-Malinici I, Gohil M, Lundh S et al (2018) Determinants of response and resistance to CD19 chimeric antigen receptor (CAR) T cell therapy of chronic lymphocytic leukemia. Nat Med 24:563–571
30. Tan A C, Ashley D M, Lopez G Y, Malinzak M, Friedman H S, Khasraw M (2020) Management of glioblastoma: state of the art and future directions. CA Cancer J Clin.

31. Zamarin D, Palese P (2012) Oncolytic Newcastle disease virus for cancer therapy: old challenges and new directions. Future Microbiol 7:347–367
32. Curtsinger JM, Valenzuela JO, Agarwal P, Lins D, Mescher MF (2005) Type I IFNs provide a third signal to CD8 T cells to stimulate clonal expansion and differentiation. J Immunol 174:4465–4469
33. Zhao Z, Condomines M, van der Stegen SJC, Perna F, Kloss CC, Gunset G et al (2015) Structural design of engineered costimulation determines tumor rejection kinetics and persistence of CAR T cells. Cancer Cell 28:415–428
34. Pikor LA, Bell JC, Diallo JS (2015) Oncolytic viruses: exploiting cancer's deal with the devil. Trends Cancer 1:266–277
35. Son DS, Kabir SM, Dong Y, Lee E, Adunyah SE (2013) Characteristics of chemokine signatures elicited by EGF and TNF in ovarian cancer cells. J Inflamm (Lond) 10:25
36. Nagarsheth N, Wicha MS, Zou W (2017) Chemokines in the cancer microenvironment and their relevance in cancer immunotherapy. Nat Rev Immunol 17:559–572
37. Di Paolo NC, Miao EA, Iwakura Y, Murali-Krishna K, Aderem A, Flavell RA et al (2009) Virus binding to a plasma membrane receptor triggers interleukin-1 alpha-mediated proinflammatory macrophage response in vivo. Immunity 31:110–121
38. Prestwich RJ, Errington F, Diaz RM, Pandha HS, Harrington KJ, Melcher AA et al (2009) The case of oncolytic viruses versus the immune system: waiting on the judgment of Solomon. Hum Gene Ther 20:1119–1132
39. Kanerva A, Nokisalmi P, Diaconu I, Koski A, Cerullo V, Liikanen I et al (2013) Antiviral and antitumor T-cell immunity in patients treated with GM-CSF-coding oncolytic adenovirus. Clin Cancer Res 19:2734–2744
40. Schietinger A, Philip M, Liu RB, Schreiber K, Schreiber H (2010) Bystander killing of cancer requires the cooperation of CD4(+) and CD8(+) T cells during the effector phase. J Exp Med 207:2469–2477
41. Guedan S, Alemany R (2018) CAR-T cells and oncolytic viruses: joining forces to overcome the solid tumor challenge. Front Immunol 9:2460
42. Shultz LD, Ishikawa F, Greiner DL (2007) Humanized mice in translational biomedical research. Nat Rev Immunol 7:118–130
43. Zhu G D, Zhang Q, Zhang J W, Liu F S (2021) Targeting tumor-associated antigen: a promising CAR-T therapeutic strategy for glioblastoma treatment. Front Pharmacol. 12